IOP Publishing Journal of Optics
J. Opt. 18 (2016) 125004 (7pp) doi:10.1088/2040-8978/18/12/125004

Graphene plasmons embedded in a gain medium: layer and ribbon plasmons

Galaad Altares Menendez, Gilles Rosolen and Bjorn Maes

Micro- and Nanophotonic Materials Group, Faculty of Science, University of Mons, 20 Place du Parc, B-7000 Mons, Belgium

E-mail: Galaad.AltaresMenendez@umons.ac.be

Received 6 July 2016, revised 25 August 2016
Accepted for publication 16 September 2016
Published 2 November 2016

Abstract

Graphene plasmonics has attracted much attention due to its remarkable properties such as tunable conductivity and extreme confinement. However, losses remain one of the major drawbacks to developing more efficient devices based on graphene plasmons. Here we show that when a gain medium is introduced around a 1D graphene sheet, lossless propagation can be achieved for a critical gain value. Both numerics and analytics are employed; and with the Drude approximation the analytical expression for this critical gain becomes remarkably simple. Furthermore, we examine a single 2D graphene nanoribbon within a gain environment. We report that the plasmonic resonant modes exhibit a spasing effect for a specific value of the surrounding gain. This feature is indicated by an absorption cross section that strongly increases and narrows. Finally, we manage to connect the ribbon results to the 1D sheet critical gain, by taking external coupling into account.

Keywords: plasmonics, graphene, nanoribbon

(Some figures may appear in colour only in the online journal)

1. Introduction

Graphene is a two-dimensional hexagonal lattice of carbon atoms, which behaves as a metallic layer at mid-infrared frequencies. As a result, plasmonic modes guided by graphene sheets have been predicted and demonstrated [1, 2], and they exhibit a remarkable sub-wavelength confinement [3]. Therefore they constitute a promising alternative to metallic thin layers [4] and have been used for complete optical absorption [5], tunable metasurfaces [6] and many other applications. However, due to the well-known trade-off between confinement and dissipative losses in plasmonic devices, one cannot achieve very long propagation lengths [7, 8]. Therefore, remedies are required to compensate the losses, in order to enhance the technological potential for applications.

Specific solutions to this problem are e.g. to improve fabrication methods to minimize dissipative losses in graphene [9], or to use heterostructures such as graphene with boron nitride, wherein hybrid modes suffer from less losses [10]. Another solution, which we study here, is to introduce a gain medium adjacent to graphene in order to compensate the losses.

Gain compensation of surface plasmons in 'traditional' metallic structures has been investigated [11]. A popular solution is to use an active dielectric medium close to the metal, which can achieve an increased scattering cross section for metallic nanoparticles [12] and lossless propagation for specific gain values in plasmonic devices [13, 14]. Using resonant plasmonic structures and a gain medium, spasers [15] have been demonstrated [16], and are a valuable source of intense optical fields localized on the nanoscale.

Other works also investigated solutions to overcome losses in graphene plasmonic structures by optically pumping the graphene [17, 18], by combining it with resonant metallic structures [19, 20] or by using PT-symmetric schemes [21]. Graphene nanoflakes coupled to optically excited carbon nanotubes have been proposed [22] and are shown to exhibit a spasing behaviour for carefully chosen structural parameters.

In this work we use analytical models and rigorous finite element method (FEM) simulations to show that the introduction of a gain medium in the vicinity of graphene sheets

can lead to loss compensation. We also show that two-dimensional (2D) graphene ribbons surrounded by a gain medium exhibit an enhanced absorption cross section. This behaviour leads to a spasing effect for a specific gain value, which we connect with the loss compensation model previously introduced for the one-dimensional (1D) graphene sheets. The phenomena in both geometries (1D sheets and 2D ribbons) are thus connected and are well described by approximate, insightful analytical relations.

We first introduce general graphene plasmon concepts in section 2. Section 3 introduces how a gain medium surrounding a graphene sheet can lead to improved propagation lengths, using analytical models and simulations with COMSOL Multiphysics, a commercial finite element based software package. Finally in section 4 we study graphene ribbons, and show that the extinction cross section of graphene ribbons is dramatically improved, leading to spasing modes by tuning the gain medium surrounding those ribbons. Finally, we connect the results for 1D graphene sheets to those for 2D ribbon structures.

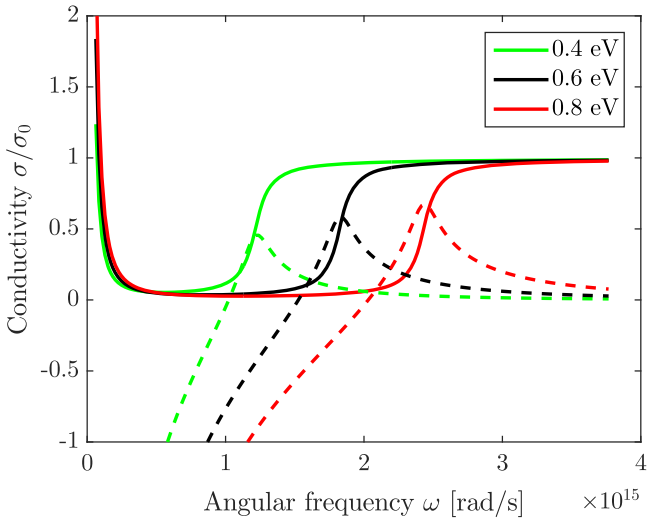

Figure 1. Real (solid lines) and imaginary part (dashed lines) of the conductivity (equation (1)) for several values of graphene doping E_F (0.4, 0.6 and 0.8 eV). The conductivity values are normalized by the constant $\sigma_0 = e^2/(4\hbar)$.

2. Graphene plasmons

Before introducing gain we first describe the lossy modes. In order to derive the graphene plasmon (GP) dispersion relation, one can model the graphene sheet by a plane with a dispersive conductivity $\sigma(\omega)$ containing two main contributions: one from the intraband electronic transitions (σ_{intra}) and one from the interband electronic transitions (σ_{inter}). These contributions are expressed as follows in the case where the graphene doping level $E_F \gg k_B T \approx 0.026$ eV at room temperature [23, 24]:

$$\sigma(\omega) = \sigma_{\text{intra}}(\omega) + \sigma_{\text{inter}}(\omega) \tag{1}$$

$$\sigma_{\text{intra}}(\omega) = \frac{e^2 E_F}{\pi\hbar^2}\frac{-i}{\omega - i\tau^{-1}} \tag{2}$$

$$\sigma_{\text{inter}} = \frac{e^2}{4\hbar}\left\{\frac{1}{2} + \frac{1}{\pi}\arctan\left[\frac{\hbar\omega - 2E_F}{2k_B T}\right]\right\} + \frac{e^2}{4\hbar}\left\{\frac{i}{2\pi}\ln\left[\frac{(\hbar\omega + 2E_F)^2}{(\hbar\omega - 2E_F)^2 + (2k_B T)^2}\right]\right\} \tag{3}$$

where $\tau = 0.16$ ps [25] accounts for electron scattering. The total conductivity $\sigma(\omega)$ is shown in figure 1 for several values of E_F. At low frequencies, the conductivity is dominated by σ_{intra}, while at higher frequencies σ_{inter} becomes significant.

To describe mode propagation along z we use the convention $\exp[-i\beta z]$. A graphene sheet can be modelled with a surface current using equation (1), and solving Maxwell's equations leads to the dispersion relation for the GP propagation constant β [3]:

$$\beta = \pm\sqrt{\varepsilon_r k_0^2 - \frac{4\omega^2\varepsilon_0^2\varepsilon_r^2}{\sigma^2(\omega)}} \tag{4}$$

where ε_0 is the vacuum permittivity, ε_r is the relative permittivity of the medium surrounding the graphene sheet, and $k_0 = \omega/c$. The sign of β gives the propagation direction along the z axis. We choose the minus sign so that $\Re(\beta) > 0$ and the plasmonic mode propagates towards positive z values. In this paper we consider the nonretarded regime where $\beta \gg k_0$, the dispersion relation of equation (4) then becomes

$$\beta = \frac{-2i\omega\varepsilon_0\varepsilon_r}{\sigma(\omega)}. \tag{5}$$

This relation can be used to derive various characteristics of GPs, such as their lateral confinement or their propagation length $L = 1/[2\Im(\beta)]$. One can see that the propagation length becomes infinite if the imaginary part of the propagation constant $\Im(\beta)$ vanishes. In the next section we explain how this can be achieved using a gain medium.

3. Critical gain in 1D structures

We now show how losses can be entirely compensated using a gain medium surrounding the graphene sheet. We assume that the gain medium is described by its relative permittivity $\varepsilon_r = \varepsilon_R - i\varepsilon_I$. With this convention a medium with $\Im(\varepsilon_r) > 0$ is a gain medium and a mode with a propagation constant β such that $\Im(\beta) > 0$ is amplified along its propagation direction. In practice, such a gain medium could consist of a quantum cascade gain medium [26], of a nonlinear medium used for frequency mixing [27], or of other pumped gain elements such as carbon nanotubes [22]. A typical plasmonic mode supported by a graphene sheet is shown in figure 2. This mode is tightly confined around the sheet, as its amplitude rapidly vanishes as a function of the distance to the sheet.

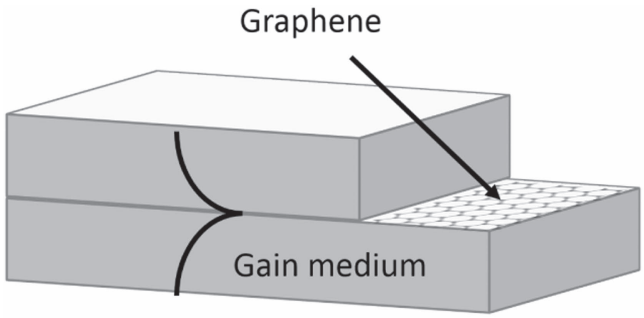

Figure 2. Schema of the structure under investigation: a graphene sheet lays between two semi-infinite layers of a gain medium. We study the properties of the plasmonic mode supported by the graphene sheet while we vary the gain medium permittivity.

Using equation (5) one finds that $\Im(\beta) = 0$ (so the propagation length L becomes infinite) for $\varepsilon_I = \varepsilon_{I\text{crit}}$ where

$$\varepsilon_{I\text{crit}} = \varepsilon_R \frac{\Re[\sigma(\omega)]}{\Im[\sigma(\omega)]}. \tag{6}$$

To get further insight into the parameter dependencies hidden in $\sigma(\omega)$, we assume the Drude-like approximation: when doping and wavelength are large, i.e. for $\hbar\omega \ll 2E_F$, the interband contribution disappears (see equation (2)) and the conductivity of graphene reduces to equation (2) [23]. Injecting equation (2) into equation (5), one finds:

$$\Re(\beta) = \frac{2\varepsilon_0\pi\hbar^2}{e^2E_F}(\varepsilon_R\omega^2 - \varepsilon_I\tau^{-1}\omega) \tag{7}$$

$$\Im(\beta) = \frac{2\varepsilon_0\pi\hbar^2}{e^2E_F}(-\varepsilon_I\omega^2 - \varepsilon_R\tau^{-1}\omega). \tag{8}$$

These relations are represented for several values of gain $\Im(\varepsilon_r) = -\varepsilon_I$ in figures 3(a) and (b) (red curves) and compared to the exact solution with exact conductivity of equation (4) (green curves). The real part of the propagation constant $\Re(\beta)$ (figure 3(a)) is practically independent of the surrounding gain. On the other hand, the imaginary part $\Im(\beta)$ (figure 3(b)) strongly depends on the surrounding gain. For a sufficiently large value of gain, $\Im(\beta)$ becomes positive and GPs are amplified.

We also show results with rigorous FEM simulations in figure 3 (blue dotted lines). In these simulations, graphene is modelled by a current line that possesses a conductivity described in equation (1). The exact model (equation (4)) and the simulations are in very good agreement.

At higher frequencies it may seem that the dispersion relation is not correctly described by equations (7) and (8) (via the Drude model); there is a discrepancy between results based on the Drude conductivity and the full conductivity (respectively red and green curves) at high frequencies. The Drude approximation is more accurate for $\hbar\omega \ll 2E_F$, as indeed the interband term of the conductivity (equation (2) and figure 1) decreases for smaller omega. This is why there is an increasing difference between the two results at higher frequencies. This difference is reduced for higher doping levels because then the interband term becomes smaller (see

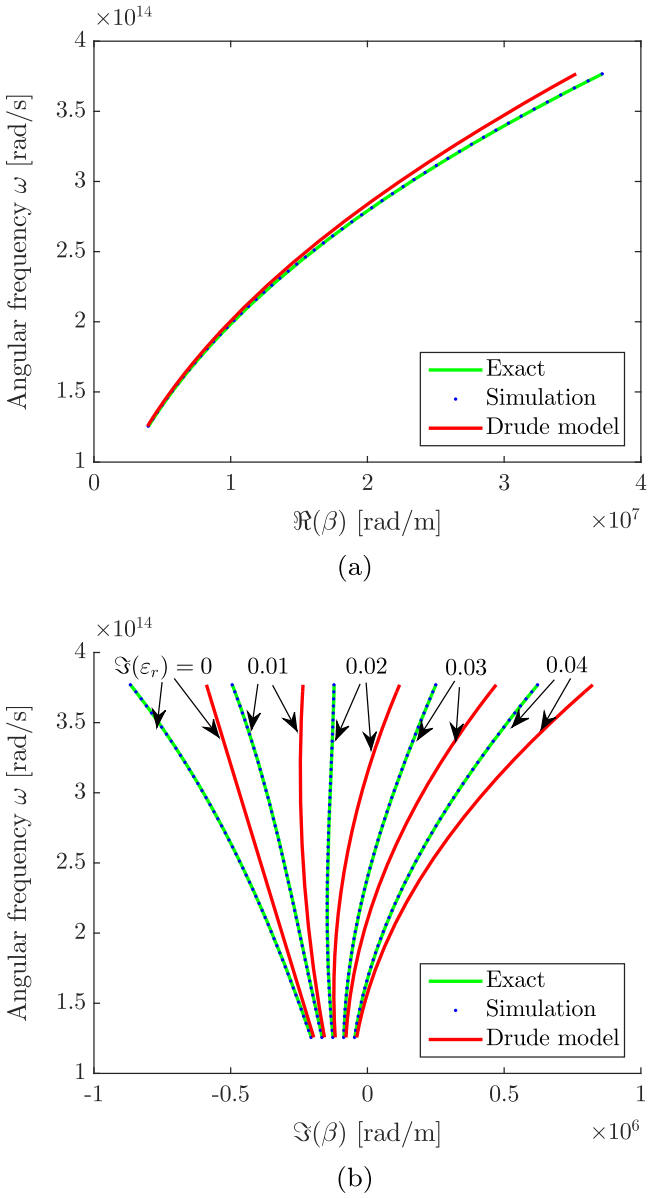

Figure 3. Dispersion of (a) $\Re(\beta)$ and (b) $\Im(\beta)$ for $\Im(\varepsilon_r) = 0$, 0.01, 0.02, 0.03, 0.04 and $E_F = 0.6$ eV. We consider a free standing graphene sheet so $\varepsilon_R = 1$. The green curve shows the analytical form with full conductivity (equation (4)), the dots are simulation results (also with full conductivity) and the red curves are equations (7) and (8) that only use the Drude conductivity. The Drude approximation is more accurate for high frequencies because the interband term of the exact conductivity is smaller. The surrounding gain medium bends $\Im(\beta)$ towards positive values.

figure 1). The interband contribution increases the dissipative losses and shifts the exact curve towards negative $\Im(\beta)$ (figure 3(b)).

Examining the two terms of equation (8) (obtained via the Drude model) is enlightening. When the surrounding gain increases (when ε_I becomes more negative), the ω^2 term becomes more important and bends the dispersion towards positive values (figure 3(b)). The term with ω is a straight line with a constant slope $-\varepsilon_R\tau^{-1}$, which drives $\Im(\beta)$ towards negative (lossy) values. An increase in τ^{-1} (in the ω term) means increased losses due to electron scattering in graphene,

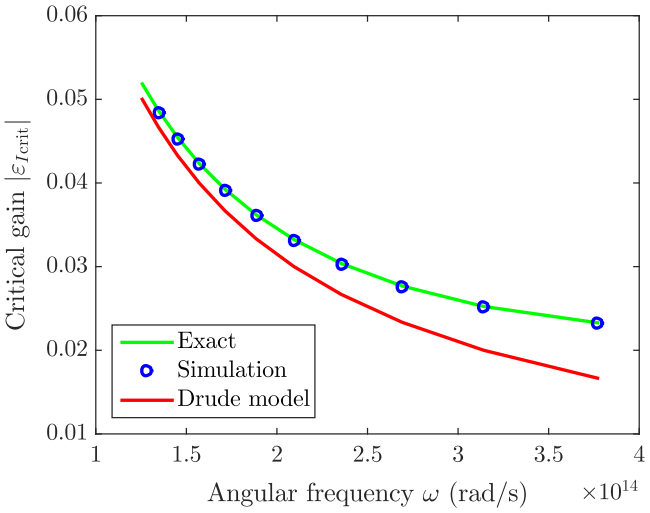

Figure 4. Comparison between critical gain values from equation (6) (green), equation (9) (red) and simulations (blue circles) for graphene sheet plasmon modes ($E_F = 0.6$ eV). This is the gain needed to compensate plasmonic losses in a graphene layer according to different approximations.

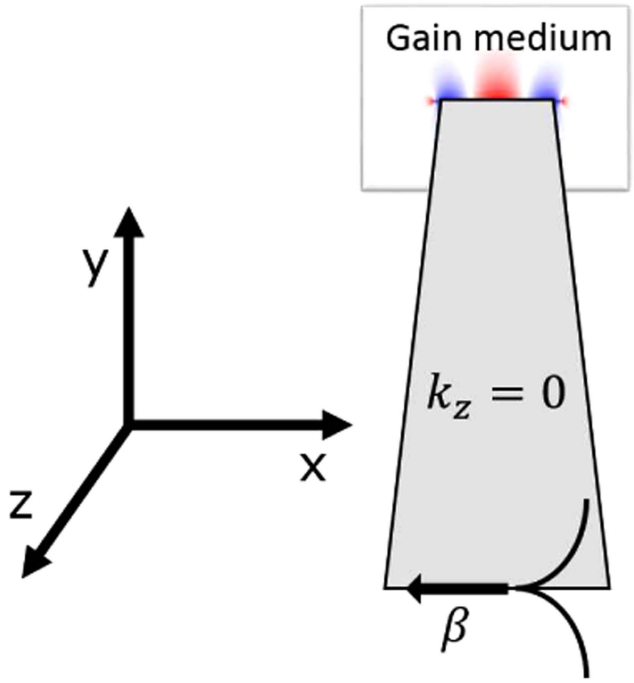

Figure 5. Graphene ribbon embedded in a gain medium, with an example of a supported mode profile (E_x for $m = 2$). A GP mode that will make round-trips for a resonance is sketched. The gain medium is a box sufficiently large to fully enclose the plasmonic mode.

and thus more losses for the GP mode. An increase in ε_R (also in the ω term) makes the GP mode more confined around the graphene sheet, and this confinement also increases losses.

From equation (8) the condition $\Im(\beta) = 0$ is achieved for a particular value of gain with an expression that is remarkably simple:

$$\varepsilon_{I\text{crit}} = \frac{-\varepsilon_R}{\omega\tau}. \tag{9}$$

Thus if the (real part of the) permittivity of the surrounding medium ε_R increases, the gain $\varepsilon_{I\text{crit}}$ needed to compensate the GP losses will also increase. This is due to the stronger confinement of the GP mode around the graphene sheet, leading to more losses. The critical gain $\varepsilon_{I\text{crit}}$ increases if the electron scattering time τ in the graphene sheet decreases. This critical gain also depends on the frequency: if ω increases, the mode is more confined around the graphene sheet as the vacuum wavelength decreases, leading to more absorption in graphene. One should note that the value of τ needs to be carefully chosen since it depends on the quality of the graphene sheet and on the doping level. Throughout this paper we mainly consider a doping value of $E_F = 0.6$ eV therefore we do not take this dependence into account. However this is no longer the case if one works with varying E_F.

Figure 4 shows the comparison between the analytical results for the critical gain $\varepsilon_{I\text{crit}}$ with full conductivity (equation (6), green line), the simulation results (also with full conductivity, blue circles), and the analytical results using only the Drude term (equation (9), red line). While the exact model describes the simulation results precisely, the Drude approximation is not perfectly accurate (for the reasons mentioned previously), but it is a useful simplification.

4. Resonant gain in 2D graphene ribbons

We now consider a ribbon of graphene, a 2D geometry. Such structures have already been studied, both for individual ribbons [28] and in periodic structures [5], the latter case potentially leading to complete optical absorption. Here the individual graphene ribbon of width D (figure 5) is embedded in a gain medium. We consider plasmonic stationary modes invariant along the ribbon, meaning that we only consider modes with a vanishing propagation constant parallel to the ribbon edges ($k_z = 0$). These stationary resonances exist if the following round-trip condition is fulfilled [29, 30]:

$$2\beta D + 2\Phi_R = 2\pi m \tag{10}$$

where β is the 1D sheet propagation constant (discussed before, see equation (4)), $\Phi_R = -0.75\pi$ is the (non-trivial) phase reflection at a ribbon edge, and m is the mode order.

Using this straightforward model we can predict that the resonance frequencies of a ribbon are given by

$$\omega_m = \frac{-\Im[\sigma(\omega)](m\pi - \Phi_R)}{2\varepsilon_0\varepsilon_r D}. \tag{11}$$

We are again interested in a simpler expression, by using the Drude model, so introducing equation (2) into equation (11), we find

$$\omega_m = \frac{e}{\hbar}\sqrt{\frac{E_F(m\pi - \Phi_R)}{2\varepsilon_0\varepsilon_r \pi D}}. \tag{12}$$

We first simulate the absorption cross section σ_{abs}/L (where L is the normalizing z-length of the ribbon) of a

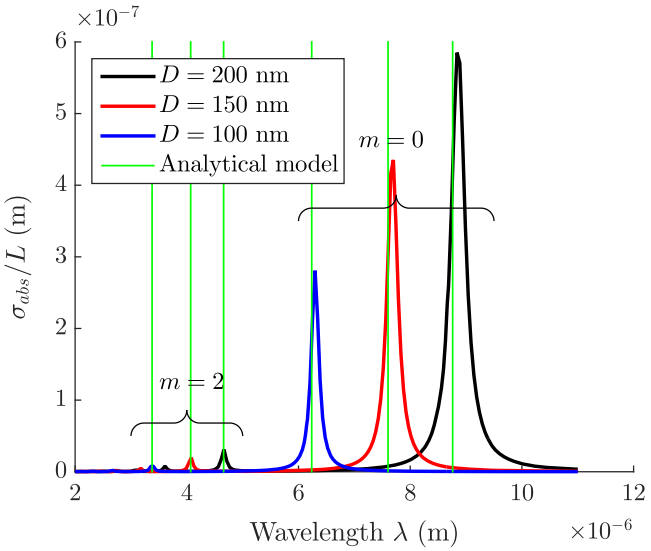

Figure 6. Absorption spectrum of a graphene free standing ribbon obtained via FEM simulations for $D = 100$, 150 and 200 nm with $E_F = 0.6$ eV. Vertical green lines represent the peak positions predicted by equation (11) for $m = 0$ and $m = 2$ (only even modes are excited because of the parity of the incident light).

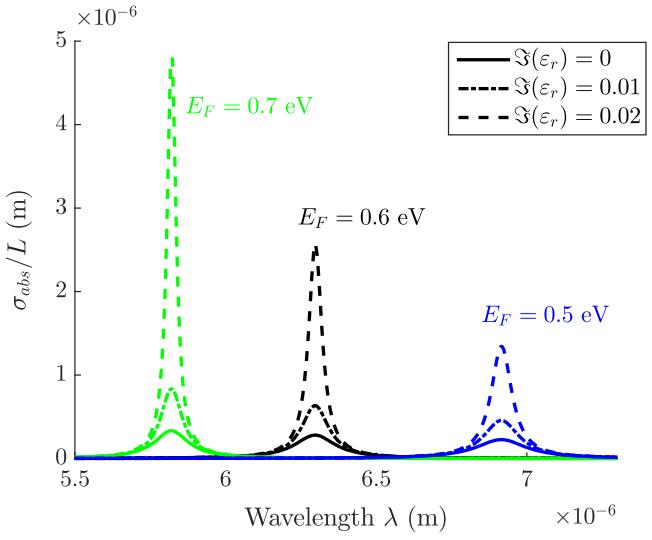

Figure 7. Absorption cross section of a 100 nm graphene ribbon ($E_F = 0.5$, 0.6 and 0.7 eV) for several values of the surrounding gain: $\Im(\varepsilon_r) = 0$, 0.01, 0.02. A higher E_F gives a higher resonance frequency ω_m (equation (12)) while the surrounding gain strongly changes the peaks' height and width.

graphene ribbon [31] without gain around (figure 6). These results are obtained by sending a TM polarized plane wave with $\vec{H}$ parallel to the z-axis at normal incidence onto the ribbon. The simulated structure is a graphene ribbon surrounded by a gain medium (a box sufficiently large so the plasmonic mode is fully enclosed in it). The boundary of this structure is a PML cylinder sufficiently distant from the gain box. To compute the absorption cross section, we measured the fraction of power absorbed by the graphene ribbon P_{abs} and normalized it by the power flux P_0 of the normally incident plane wave so the normalized absorption cross section is given by $\sigma_{\text{abs}}/L = P_{\text{abs}}/P_0$.

Simulated peak positions are in good agreement with equation (11) (green vertical lines in figure 6). In more detail, table 1 shows a comparison between equation (11) and the simulations. The small difference between these two values could be accounted for with a more precise reflection phase at the end of the ribbon.

We then introduce gain surrounding the graphene ribbons and compute the absorption cross section of the ribbon as a function of the wavelength (note that here, the extinction nearly equals absorption). Figure 7 shows these spectra for various surrounding gains and doping of the graphene ribbon. The width and maximum height of the absorption peaks strongly depends on the surrounding gain, whereas the position of the peaks remains unchanged. A straightforward analysis of equation (11) shows that the real part of ω_m is virtually independent of the gain value: the gain value only appears in a $\varepsilon_R/(\varepsilon_R^2 + \varepsilon_I^2)$ term so we can neglect the ε_I^2 contribution because there is a large difference (four orders of magnitude) between ε_R^2 and ε_I^2.

From these simulations we determine the characteristics of the absorption peaks (maximum height and full-width at half-maximum FWHM) as a function of the surrounding gain $\Im(\varepsilon_r)$. We find that for a specific value of gain, the absorption cross section is considerably enhanced and the width of the absorption peak approaches zero, as shown in figures 8(a) and (b), leading to a laser (or spaser) behaviour. These results are obtained by fitting the absorption peak from figure 6 by a Lorentzian function.

In order to connect our 2D models and simulations to the previous section dedicated to 1D graphene sheets, we compare the critical gain in both cases for several frequencies (obtained in 2D by choosing different ribbon widths, and thus resonance frequencies, varying from $D = 100$ nm to $D = 500$ nm). Remark the difference between the critical gain in 1D, which corresponds to lossless GP mode propagation, and the critical gain in 2D, which corresponds to spasing behaviour. The latter critical effect is thus more comprehensive, as all losses (propagation losses of all modes and coupling losses) need to be overcome. Figure 9 shows in blue the

Table 1. Peak positions from equation (11) and FEM for several ribbon widths and mode orders. Odd modes are not excited here because of the parity of the incident light.

Order	$D = 100$ nm		$D = 150$ nm		$D = 200$ nm	
	Equation (11)	FEM	Equation (11)	FEM	Equation (11)	FEM
$m = 0$	6.24 μm	6.30 μm	7.60 μm	7.69 μm	8.76 μm	8.86 μm
$m = 2$	3.38 μm	3.38 μm	4.07 μm	4.07 μm	4.66 μm	4.67 μm

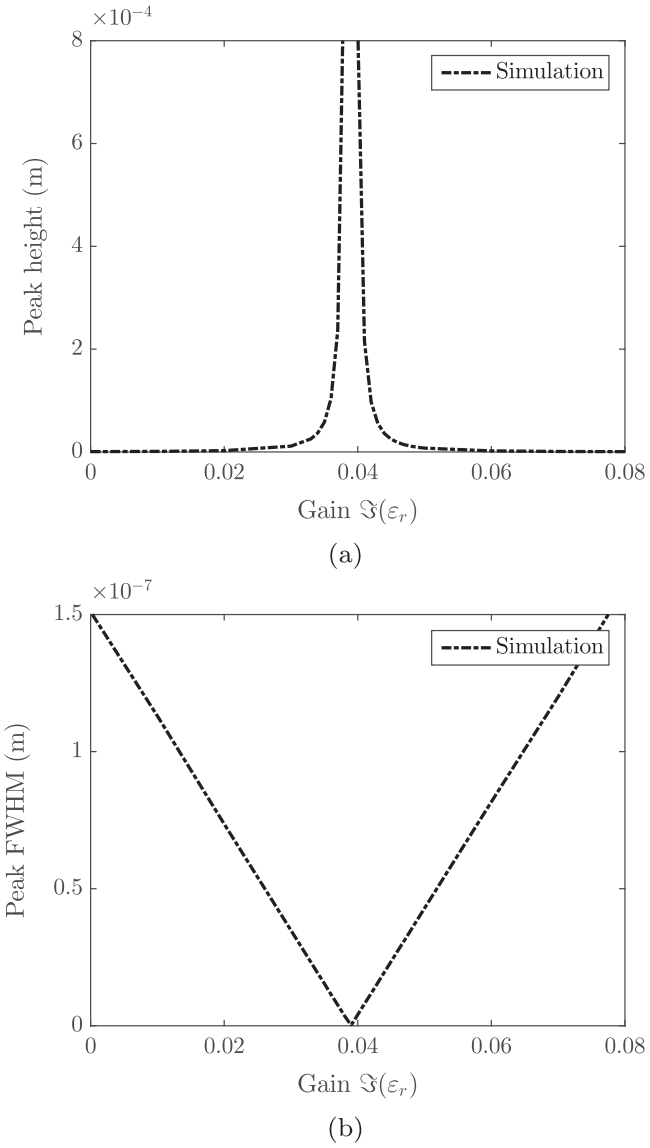

Figure 8. (a) Absorption peak height, and (b) absorption peak width as a function of surrounding gain. Ribbon parameters here are $D = 200$ nm and $E_F = 0.6$ eV, and the fit is done for the fundamental mode ($m = 0$). The absorption peak become stronger and narrower for a specific gain value.

critical gain (for spasing) for 2D ribbons as a function of their resonance frequency for mode orders $m = 0$ and $m = 2$, in green the critical gain (for a lossless mode) for 1D graphene sheets with full conductivity (equation (6)), and in red the critical gain (for a lossless mode) also for 1D graphene sheets with the Drude approximation (equation (9)).

Figure 9 shows a good agreement between simulation results for the $m = 2$ resonances and the 1D critical gain expression (equation (6)) obtained with the full conductivity. For $m = 0$ order modes however, the gain needed to compensate losses is higher in ribbons than in graphene sheets. This is because the light trapped in the lower order ($m = 0$) ribbon mode couples efficiently to outgoing radiation, in contrast with the higher order ($m = 2$) mode. Therefore the 2D critical gain is the gain needed to compensate losses in graphene (just as in graphene sheets) and, in addition, to

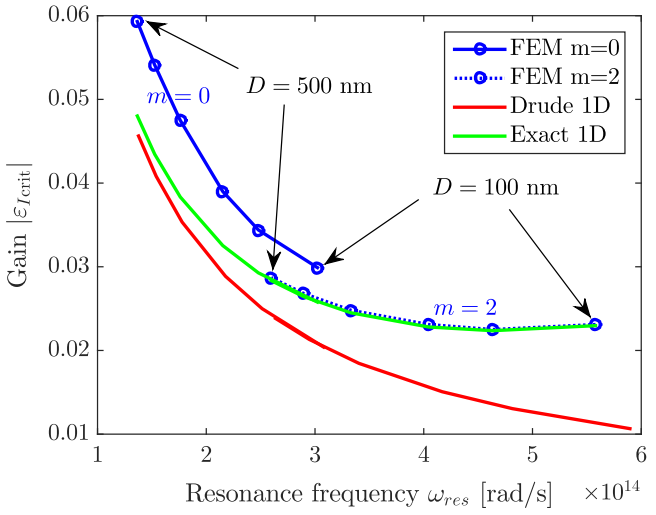

Figure 9. Critical gain as a function of the ribbon resonance frequencies for several models: in blue FEM simulations for 2D ribbon spasing (orders $m = 0$ and $m = 2$, $D = 100$, 150, 200, 300, 400 and 500 nm), in red for 1D sheets with the Drude approximation, and in green for 1D sheets with full conductivity. The simulations correspond to different ribbon widths D so that different frequencies for gain compensation are investigated.

compensate the energy lost by radiation outcoupling. Thus the critical gain in the 2D case has to surpass the one for the 1D case, when radiative coupling is important. Note that the 2D $m = 0$ and 1D critical gain (green curve) are quasi-parallel, suggesting that the outcoupling losses are fairly independent of the frequency, which seems physically plausible as coupling mainly happens via the corners and the latter effect is not strongly influenced by the ribbon width.

5. Conclusion

We studied how the introduction of a gain medium surrounding graphene sheets leads to complete compensation of graphene-induced losses in plasmonic modes. We analytically determined the critical gain value for a 1D graphene layer and checked our models via rigorous FEM simulations. The simple form of the analytical expressions for the critical gain allows for an insightful comprehension of the loss balance taking place. We illustrate this by determining how both the real and imaginary parts of the propagation wavevector β depend on the surrounding gain.

We further examined 2D graphene ribbons and showed how the extinction cross section is considerably enhanced by tuning the gain around these ribbons. We obtained a spasing behaviour for a specific gain value, indicated by a strongly increasing and narrowing peak. These 2D ribbon effects can be connected to the 1D critical gain, by taking into account that the ribbon structure includes both plasmon propagation losses and radiative losses, which are important for low order modes.

Acknowledgments

This work was supported by the Belgian Science Policy Office under the project 'Photonics@be' (P7-35) and by the Fonds pour la Formation à la Recherche dans l'Industrie et dans l'Agriculture (FRIA) in Belgium.

References

[1] Chen J *et al* 2012 Optical nano-imaging of gate-tunable graphene plasmons *Nature* **487** 77–81
[2] Grigorenko A N, Polini M and Novoselov K S 2012 Graphene plasmonics *Nat. Photon.* **6** 749–58
[3] Jablan M, Buljan H and Soljacic M 2009 Plasmonics in graphene at infrared frequencies *Phys. Rev.* B **80** 245435
[4] He X, Gao P and Shi W 2016 A further comparison of graphene and thin metal layers for plasmonics *Nanoscale* **8** 10388–97
[5] Thongrattanasiri S, Koppens F H L and Garcia de Abajo F J 2012 Complete optical absorption in periodically patterned graphene *Phys. Rev. Lett.* **108** 047401
[6] He X 2015 Tunable terahertz graphene metamaterials *Carbon* **82** 229–37
[7] Tassin P, Koschny T, Kafesaki M and Soukoulis C M 2012 A comparison of graphene, superconductors and metals as conductors for metamaterials and plasmonics *Nat. Photon.* **6** 259–64
[8] Tassin P, Koschny T and Soukoulis C M 2013 Graphene for terahertz applications *Science* **341** 620–1
[9] Dubrovkin A M, Tao J, Chao Yu X, Zheludev N I and Jie Wang Q 2015 The reduction of surface plasmon losses in quasi-suspended graphene *Sci. Rep.* **5** 9837
[10] Dai S *et al* 2015 Graphene on hexagonal boron nitride as a tunable hyperbolic metamaterial *Nat. Nanotechnol.* **10** 682–6
[11] Berini P and De Leon I 2011 Surface plasmon-polariton amplifiers and lasers *Nat. Photon.* **6** 16–24
[12] Lawandy N M 2004 Localized surface plasmon singularities in amplifying media *Appl. Phys. Lett.* **85** 5040
[13] Nezhad M P, Tetz K and Fainman Y 2004 Gain assisted propagation of surface plasmon polaritons on planar metallic waveguides *Opt. Express* **12** 4072
[14] Noginov M A, Podolskiy V A, Zhu G, Mayy M, Bahoura M, Adegoke J A, Ritzo B A and Reynolds K 2008 Compensation of loss in propagating surface plasmon polariton by gain in adjacent dielectric medium *Opt. Express* **16** 1385
[15] Bergman D J and Stockman M I 2003 Surface plasmon amplification by stimulated emission of radiation: quantum generation of coherent surface plasmons in nanosystems *Phys. Rev. Lett.* **90** 027402
[16] Stockman M I 2011 Nanoplasmonics: past, present, and glimpse into future *Opt. Express* **19** 22029
[17] Dubinov A A, Aleshkin V Y, Mitin V, Otsuji T and Ryzhii V 2011 Terahertz surface plasmons in optically pumped graphene structures *J. Phys.: Condens. Matter* **23** 145302
[18] Hamm J M, Page A F, Bravo-Abad J, Garcia-Vidal F J and Hess O 2016 Nonequilibrium plasmon emission drives ultrafast carrier relaxation dynamics in photoexcited graphene *Phys. Rev.* B **93** 041408
[19] Takatsuka Y, Takahagi K, Sano E, Ryzhii V and Otsuji T 2012 Gain enhancement in graphene terahertz amplifiers with resonant structures *J. Appl. Phys.* **112** 033103
[20] Popov V V, Polischuk O V, Davoyan A R, Ryzhii V, Otsuji T and Shur M S 2012 Plasmonic terahertz lasing in an array of graphene nanocavities *Phys. Rev.* B **86** 195437
[21] Lin X, Li R, Gao F, Li E, Zhang X, Zhang B and Chen H 2016 Loss induced amplification of graphene plasmons *Opt. Lett.* **41** 681
[22] Rupasinghe C, Rukhlenko I D and Premaratne M 2014 Spaser made of graphene and carbon nanotubes *ACS Nano* **8** 2431–8
[23] Falkovsky L A and Varlamov A A 2007 Space–time dispersion of graphene conductivity *Eur. Phys. J.* B **56** 281–4
[24] Falkovsky L A 2008 Optical properties of graphene *J. Phys.: Conf. Ser.* **129** 012004
[25] Novoselov K S 2004 Electric field effect in atomically thin carbon films *Science* **306** 666–9
[26] Yao Y, Hoffman A J and Gmachl C F 2012 Mid-infrared quantum cascade lasers *Nat. Photon.* **6** 432–9
[27] Chui H C, Woods G L, Fejer M M, Martinet E L and Harris J S 1995 Tunable mid-infrared generation by difference frequency mixing of diode laser wavelengths in intersubband InGaAs/AlAs quantum wells *Appl. Phys. Lett.* **66** 265
[28] Christensen J, Manjavacas A, Thongrattanasiri S, Koppens F H L and Garcia de Abajo F J 2012 Graphene plasmon waveguiding and hybridization in individual and paired nanoribbons *ACS Nano* **6** 431–40
[29] Nikitin A Y, Low T and Martin-Moreno L 2014 Anomalous reflection phase of graphene plasmons and its influence on resonators *Phys. Rev.* B **90** 041407
[30] Rosolen G and Maes B 2014 Nonuniform doping of graphene for plasmonic tapers *J. Opt.* **17** 015002
[31] Garcia de Abajo F J 2014 Graphene plasmonics: challenges and opportunities *ACS Photonics* **1** 135–52